

CELLO: AN ADVANCED LBIC MEASUREMENT TECHNIQUE FOR SOLAR CELL LOCAL CHARACTERIZATION

J. CARSTENSEN, G. POPKIROV, J. BAHR, H. FÖLL
Faculty of Engineering
Christian-Albrechts University of Kiel, Kaiserstr. 2, D-24143 Kiel, Germany

1. Introduction

A solar cell is a large area device, thus its global IV-characteristic and efficiency strongly depend on local properties. The existence of local defects, such as locally decreased diffusion length, strong local shunt- or high local series resistances, will adversely influence the solar cell global properties. Experimental techniques suitable to map the spatial distribution of such local parameters can provide valuable information and thus help to improve the technology for production of efficient and reproducible solar cells. The LBIC (Light Beam Induced Current) technique [1] allows the calculation of the local diffusion length of the solar cell material from local photo current data obtained at short-circuit condition. The mapping analyzer PVScan 5000 by NREL [2] can be used additionally to LBIC, to map defects and grain boundaries using reflectivity data, and special surface etching. Localized shunts can be mapped by CCD-cameras [3,4] or nematic liquid crystals [5]. Electron-beam-induced current (EBIC) is an alternative technique for the investigation of defects in solar cells [6]. Destructive techniques, MASC [7] for local IV-characterization and RAMP [8] using a scanning (by scratching) tungsten electrode were developed recently.

The aim of this paper is to describe a new advanced LBIC measurement technique, called 'CELLO' (solar CELl LOcal characterization) which allows the determination of all local parameters, especially the local series- and shunt resistance, $R_s(x,y)$ and $R_{sh}(x,y)$, and thus to identify all material- and process-induced, efficiency relevant defects. In principle, the data obtained could also be used to simulate the behavior of the complete solar cell for any set of technology parameters.

2. The measurement technique

A simplified schematic diagram of CELLO is depicted in Fig. 1. The solar cell is illuminated homogeneously by a set of halogen lamps with near to 1.5 AM intensity. Additionally, an intensity modulated infrared laser beam focussed to about 100 μ m diameter is scanning the sample using piezo-controlled mirrors allowing for high resolution maps of the local linear responds. A home-made, computer controlled, low noise potentiostat/galvanostat is used for voltage/current control and current/voltage measurement with high S/N ratio. A lock-in amplifier, synchronized to the laser beam

modulation signal, is used to measure the solar cell response to the laser beam perturbation. The CELLO technique measures the solar cell global response $dI(U_{cell,x,y})$ and $dU(I_{cell,x,y})$ to local perturbations as shown in Fig. 2. The data obtained are fitted to a complete (and partially novel) model of the solar cell which allows: i) to draw solar cell surface maps of the measured data, ii) to calculate maps of the local series- and

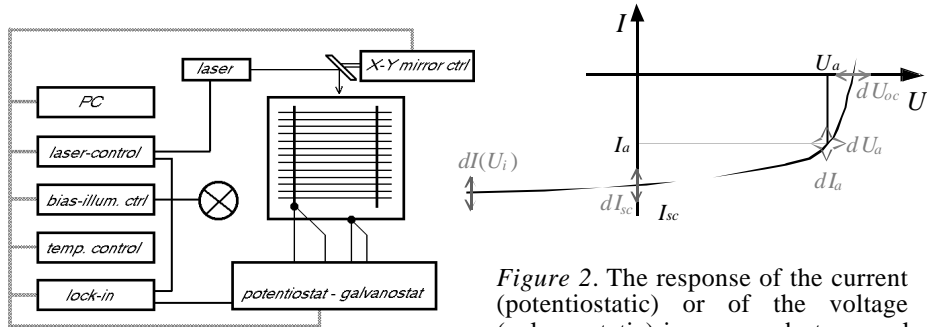


Figure 1. Block scheme of the CELLO

Figure 2. The response of the current (potentiostatic) or of the voltage (galvanostatic) is measured at several points along the IV curve.

shunt resistances, diffusion length and back-surface field, and iii) to construct the complete local IV-curve for each point at the solar cell. In this context, the well known LBIC mode is just the measurement at $U_{cell}=0$.

3. Modeling and calculations

If sufficient data sets have been obtained experimentally, the raw data can be converted into local parameters of the solar cell. This is done with the help of the equivalent circuit as shown in Fig. 3. The solar cell is divided in a global part and a local part which are described by different sets of parameters. The global part is just the constant IV-curve of the complete solar cell. In a linear response approach any small local illumination can be added with a proper local set of solar cell parameters without changing the global values when assuming that the interconnect (the grid) between the complete

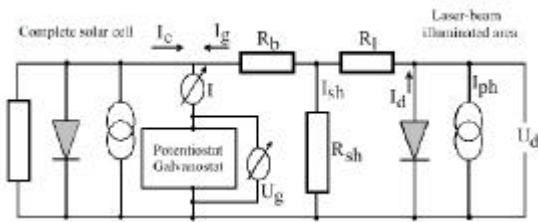


Figure 3. Equivalent circuit

solar cell and the additionally illuminated area serves as an equipotential layer. There are two important modifications in the equivalent circuit shown in Fig. 3 with respect to conventional diagrams: i) the two parts of the cell are connected via two resistors as shown, ii) the combination of the local diode and the local current source (laser induced photo current) is not described by the usual equations, but couples the diode current I_d and the generated, and collected photo currents I_{ph} and I_{ph0} for any given point on the

solar cell surface via $I_{ph} = I_{ph,0} - C_{rec}I_d^3$. Here, $C_{rec}I_d^3$ represents the current due to local recombination losses with C_{rec} as a fit parameter. This equation describes the lateral diffusion and recombination of minorities and expresses a sensitivity of the solar cell to gradients of the diffusion length. In fact, not all carriers, photo generated close to the surface are collected and contribute to the current at finite values of the voltage. Some carriers experience recombination in areas laterally removed from their respective point of origin. Thus, if the local diffusion length varies significantly in the lateral direction, this will influence the local properties of the point on the solar cell under consideration. It follows that the average diffusion length of a solar cell material is not a sufficient measure of the local recombination activity. The gradients in the diffusion length distribution are just as important. The complete set of equations (grid is an equipotential surface) is

$$I_g = I_d + I_{sh} + I_{ph} \quad (1)$$

$$I_d = I_{d1} \left[e^{\frac{qU_d}{n_1 kT}} - 1 \right] + I_{d2} \left[e^{\frac{qU_d}{n_2 kT}} - 1 \right] \quad (2)$$

$$U_g = R_{sh} I_{sh} + R_b I_g \quad (3)$$

Here, k is the Boltzmann constant, T is the temperature, q is the electron charge, I_{d1} , n_1 , and I_{d2} , n_2 are the saturation currents and ideality factors of the two diodes respectively. R_b is the lateral resistance of the emitter between the illuminated 'pixel' and the grid.

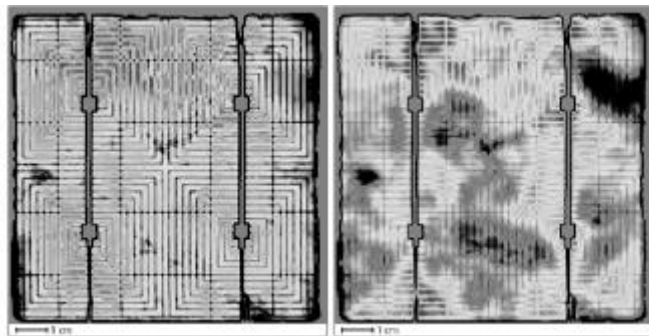


Figure 4. Maps of: dI , $U=300\text{mV}$ (left), dU , $I=300\text{mA}$ (right)

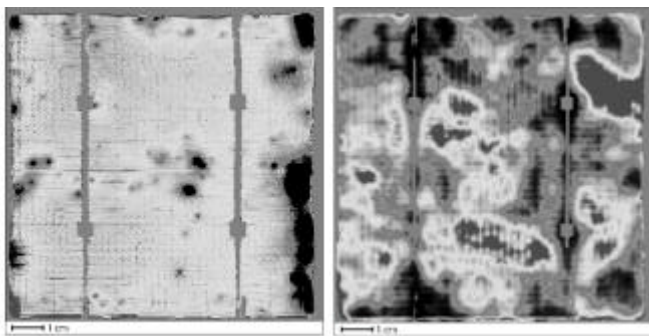


Figure 5. Maps of R_{sh} (left) and R_{ser} (right)

Photo carriers generated at one point can be collected by the grid, or get lost by recombination or via a local shunt, or. Using linear order approximations in the local laser beam induced photo current, this set of equations is generally sufficient to extract all required quantities by fitting the experimental data. The complete equivalent circuit diagram and therefore the complete set of local characteristics can be calculated from a finite set of experimental data. Local IV-curves can be calculated using data for the local shunt and

series resistances, and the local diffusion length.

4. Results

The operation of CELLO will be illustrated by some of the maps, obtained from one measurement on a solar cell, made on mc-Si wafer. Maps of the linear current response dI at $U=300\text{mV}$ and maps of the voltage response dU , measured galvanostatically at $I=300\text{mA}$ are shown in Fig.4. Fig. 5 presents calculated maps of R_{sh} and R_{ser} . We do not measure the reflectivity of the wafer with CELLO, thus we do not get information about the quantum efficiency. All other measurements are analyzed relatively to, e.g. the short circuit current. So for all other parameters local differences in the reflectivity are not important. Local IV- characteristics can be obtained from a full set of measurements fitted to the model as will be shown in a further work.

5. Conclusion

CELLO is a universal method for detecting and characterizing local defects in all solar cells since it is not restricted to silicon or crystalline materials. The measurements can provide valuable feed-back for the optimization of the process technology and materials parameters, improving efficiency and reliability of solar cells .

6. References

1. Kress, Pernau, T., Fath, P., and Bucher, E., (2000) LBIC measurements on low cost contact solar cells, *Conference proceedings, 16th European Photovoltaic Solar Energy Conversion, Glasgow, 1-5 May, 2000*, VA1.39, (File D339.pdf).
2. NREL – Technology brief (Document: NREL/MK-336-21116, 8/96)
3. D.L. King, J. A. Kratochvil, M. A Quintana., and T. J. McMahon, (2000) Applications for infrared imaging equipment in photovoltaic cell, modules and system testing, *WWW-Link: <http://www.sandia.gov/pv/ieee2000/kingquin.pdf>*.
4. M. Langenkamp, O. Breitenstein, M.E. Nell, H.-G. Wagemann, and L. Estner, (2000) Microscopic localisation and analysis of leakage currents in thin film silicon solar cell, *Conference proceedings, 16th European Photovoltaic Solar Energy Conversion , Glasgow, 1-5 May, 2000*, VD3.39 (File D411.pdf on CD version)
5. G. Färber, R.A. Bardos, K.R. McIntosh, C.B. Honsberg and A.B. Sproul, (1998) Detection of shunt resistance in silicon solar cells using liquid crystals, *Conference proceedings of the 2nd World Conference and Exhibition on Photovoltaic Solar Energy Conversion, Vienna, Austria, 6 - 10 July 1998*.
6. Boudaden, J., Riviere, A., Ballutaud, D., Muller, J.-C. and Monna, R. (2000) EBIC characterization of multicrystalline silicon solar cell emitters, *Conference proceedings, 16th European Photovoltaic Solar Energy Conversion, Glasgow, 1-5 May, 2000*, VD3.62.
7. B. Häßler, S. Thurm, W. Koch, D. Karg, G. Pensl, Conference proceedings of the 13th European Photovoltaic Solar Energy Conference, Nice, (1995) 1364.
8. A.S.H. van der Heide, A. Schönecker, G.P. Wyers, and W.C. Sinke, (2000), Mapping of contact resistance and locating shunts on solar cells using resistance analysis by mapping of potential (RAMP) technique, *Conference proceedings, 16th European Photovoltaic Solar Energy Conversion , Glasgow, 1-5 May, 2000*, VA1.60 (File D359.pdf on CD version).